Available online at www.sciencedirect.com
SCIENCE DIRECT®
Surface Science 558 (2004) 201–210
SURFACE SCIENCE
www.elsevier.com/locate/susc

Study of Fe/Mn/Fe(001) multilayers by means of scanning tunneling microscopy/spectroscopy

T.K. Yamada [a], M.M.J. Bischoff [a], A.L. Vázquez de Parga [b,*], T. Mizoguchi [c], H. van Kempen [a,*]

[a] *NSRIM, University of Nijmegen, NL-6525 ED Nijmegen, The Netherlands*
[b] *Dpto. de Física de la Materia Condensada, Universidad Autónoma de Madrid, Cantoblanco, 28049 Madrid, Spain*
[c] *Faculty of Science, Gakushuin University, 171-8588 Mejiro, Tokyo, Japan*

Received 17 September 2003; accepted for publication 7 April 2004
Available online 22 April 2004

Abstract

To elucidate the magnetic properties of a magnetic multilayer film, an understanding of the local geometry, electronic structure, and possible intermixing at the interfaces is of utmost importance. By gradually increasing the Fe coverage on the Mn(001) film, we obtained this information on the interface region by means of Auger spectroscopy and scanning tunneling microscopy/spectroscopy. Intermixed atoms and various geometries and density of states are found to exist in this system.

Keywords: Scanning tunneling microscopy; Scanning tunneling spectroscopies; Epitaxy; Growth; Iron; Manganese; Metal–metal magnetic thin film structures

1. Introduction

Due to the enormous development of the molecular beam epitaxial growth technique during the last decades, atomically flat films can be relatively easily prepared. Specially, the growth of ultra-thin magnetic multilayer films has lead to considerable practical applications such as spintronic devices: the giant magnetoresistance head, the tunnel magnetoresistance head, and the magnetoresistive random access memory [1,2].

The magnetic properties of ultrathin magnetic multilayer films are strongly affected by the local geometry, the electronic structure and possible intermixing [3,4]. Techniques like scanning electron microscopy with polarization analyzer, Kerr microscopy, spin-polarized scanning tunneling microscopy/spectroscopy make possible to study the correlation between magnetism, electronic structure, morphology, and composition [5–9]. For example, Pierce et al. studied the relation between the growth and the magnetic properties of magnetic multilayer films (Fe/[Ag,Au,Cu,Cr,Mn,V,Al]/Fe) by scanning electron microscopy with polarization analysis in a combination with reflective

* Corresponding authors. Tel.: +34-9149-74746; fax: +34-9149-73961 (A.L. Vázquez de Parga), Tel.: +31-24-365-2121; fax: +31-24-365-2190 (H. van Kempen).
E-mail addresses: al.vazquezdeparga@uam.es (A.L. Vázquez de Parga), hvk@sci.kun.nl (H. van Kempen).
URL: http://www-evsf2.sci.kun.nl/.

0039-6028/$ - see front matter © 2004 Elsevier B.V. All rights reserved.
doi:10.1016/j.susc.2004.04.004

high energy electron diffraction and scanning tunneling microscopy [5–7]. Still, there is a lack of information concerning the degree of intermixing, the crystallographic structure and the electronic structure at the interface of such multilayers at atomic level.

In the present paper we focus on the study of the growth of a magnetic multilayer by means of scanning tunneling microscopy (STM), spectroscopy (STS) and Auger spectroscopy. We studied the growth of Fe on an artificial Mn(001) surface. The Mn(001) surface was produced by depositing seven layers of pure Mn on an Fe(001) whisker. The Mn film grown in this way presents a body-centered tetragonal (bct) structure with the in-plane lattice constant dictated by the Fe whisker and an out-of-lattice constant of 0.165 nm [10]. Body-centered cubic (bcc) Fe(001) and bct Mn(001) have surface states at +0.2 and +0.8 V, respectively, which can be used for chemical identification [9,11,12].

2. Experimental

STM and STS measurements were performed in an ultra-high vacuum (UHV) chamber ($\sim 5\times 10^{-11}$ mbar) with a commercial STM (Omicron UHV STM-1) working at room temperature (RT). In this study we use W tips that were prepared as follows. A W polycrystalline wire (purity 99.99%) with a diameter of 0.5 mm was chemically etched with 5 M KOH aq., then washed with distilled water and introduced in UHV. Once in UHV the tips were sputtered with Ar^+ (1 kV) and heated by electron-bombardment (42 W).

The UHV chamber is equipped with a cylindrical mirror analyzer (PERKIN-ELMER PHI model 10–155) that allows us to do Auger electron spectroscopy measurements. The detection limit of our Auger spectroscopy was estimated to be below 1% for oxygen impurities on the Fe(001) surface, which was confirmed by atomically and chemically resolved STM images.

An Fe(001) whisker was used as a substrate [13] and was cleaned by cycles of Ar^+ sputtering (750 eV) and annealing (up to 730 °C). After this cleaning process, around 1% oxygen contaminants were measured by Auger spectroscopy and also in atomically and chemically resolved STM images [14]. In order to produce a clean Mn(001) surface about 7 mono-layers (ML) of Mn (purity 99.999%) were grown on the Fe(001) whisker which was kept at 100 °C. The evaporation rate was 0.06 nm/min. During the deposition the pressure remained below 4×10^{-10} mbar. After the deposition, more than two Mn layers were exposed on the surface. Using atomically and chemically resolved STM images we determined that, for this substrate temperature (100 °C), the intermixing between Fe and Mn is limited to the first three Mn layers. Also, the level of contaminants was below 1% on the Mn surface. Mn layers grown on Fe(001) have a bct structure with the same in-plane lattice constant as Fe(001) and an interlayer distance of 0.165 nm [10]. Theoretical calculations show that Mn(001) with a bct structure has surface states above the Fermi level that can be detected in the normalized dI/dV curves as a broad peak centered at +0.8 V [9]. Finally, Fe layers were grown on the Mn(001) surface at RT with a rate of 0.15 nm/min. Also, in this case, during the deposition the pressure remained below 3×10^{-10} mbar.

3. Results and discussion

3.1. Auger spectroscopy

Since Fe has a much higher surface energy than Mn (1.440 J/m^2 for Mn and 2.939 J/m^2 for Fe) [15], Mn is expected to segregate on top of the Fe film during the deposition. Therefore, to prevent intermixing between Mn and Fe, the Fe layers were deposited at RT. In order to test the degree of intermixing between Mn and Fe an Auger spectroscopy study was performed. During the deposition of the Fe film we moved the sample from the evaporation position to the Auger measurement position without switching off the Knudsen cell. After the Auger spectra were measured we moved the sample back to the growth position to deposit another fraction of one Fe layer.

It is well known that the mean free path for Auger electrons with energies around 40 eV is very short (3–5 atomic layers) [16]. Therefore the ratio

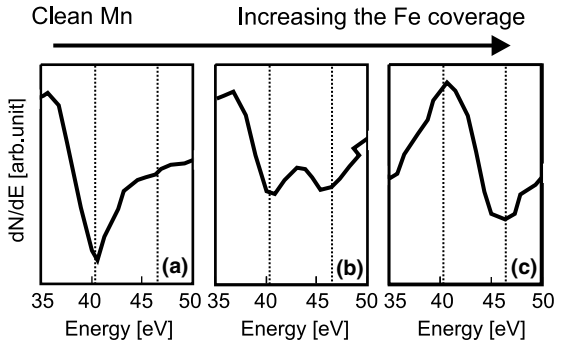

Fig. 1. Auger spectra measured on the Fe layers on a Mn(001) film in differential mode as a function of Fe coverage. From left to right the thickness of Fe is increased. The progressive appearance of the Fe(47 eV) peak and the progressive disappearance of the Mn(40 eV) peak can be observed. Dashed lines are a guide for the eyes.

between Fe(47 eV) and Mn(40 eV) peaks gives us information about the presence of Mn in the top layers of the Fe film. Fig. 1 shows the Auger spectra in a differential mode within the energy range between 35 and 50 eV for different Fe coverages. By increasing the Fe coverage the peak at 47 eV that corresponds to Fe is observed to appear gradually as the Fe thickness is increased and simultaneously the Mn peak amplitude at 40 eV is gradually lowered and finally disappears. [1] From these observations we can conclude that there is no segregation of Mn to the surface of the Fe film.

3.2. Growth of Fe on Mn(001)

Fig. 2(a) shows an STM image of the surface of 5 ML of Mn grown on the Fe(001) whisker. Four different Mn layers are exposed on the surface. Hidden Fe steps (marked with black arrows in Fig. 2(a)) and three dimensional (3D) islands produced during the Mn deposition are also observed. Details about the growth of Mn on Fe(001) and the structure of the films are given in Ref. [10]. Fig. 2(b)–(f) show topographic images obtained for different thickness of Fe grown on Mn(001).

[1] For these measurements we can only give an estimation for the Fe coverage. We estimate that the Fe thickness is below 5 ML.

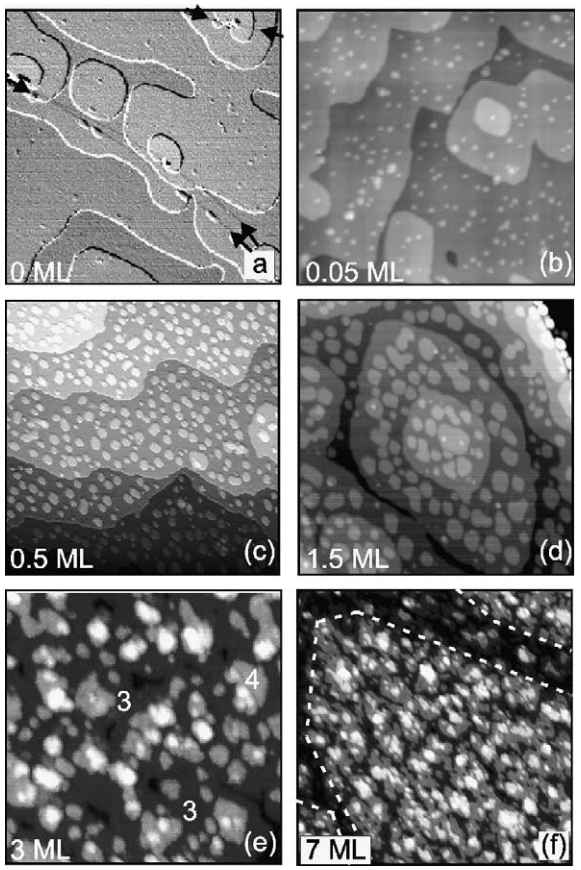

Fig. 2. STM images obtained for clean Mn(001) and for different thicknesses of Fe films grown on the Mn(001) surface at RT: (a) Mn(001) surface, 200×200 nm^2, $V_S = -0.90$ V, $I = 0.05$ nA; (b) 0.05 ML Fe, 200×200 nm^2, $V_S = -0.54$ V, $I = 0.44$ nA; (c) 0.5 ML Fe, 200×200 nm^2, $V_S = -1.00$ V, $I = 0.03$ nA; (d) 1.5 ML Fe, 200×200 nm^2, $V_S = +0.17$ V, $I = 0.19$ nA; (e) 3 ML of Fe, 55×55 nm^2, $V_S = -1.00$ V, $I = 0.04$ nA; (f) 7 ML of Fe, 100×100 nm^2, $V_S = -1.00$ V, $I = 0.03$ nA. (a) shows a topographic image in combination with a differentiation along the scanning direction. Black arrows in (a) indicate the position of the Fe hidden steps. The numbers in (e) indicate the local thickness of the Fe film. Dashed curves in (f) are guide for the eyes to mark the substrate Mn morphology.

When 0.05 ML Fe is deposited on the Mn surface, small islands appear on the surface as shown in Fig. 2(b). These islands become larger as the Fe coverage increases (Fig. 2(c)). Fig. 2(d) was obtained after the deposition of 1.5 ML of Fe. Although the Fe film follows the original morphology of the Mn(001) surface, the whole surface

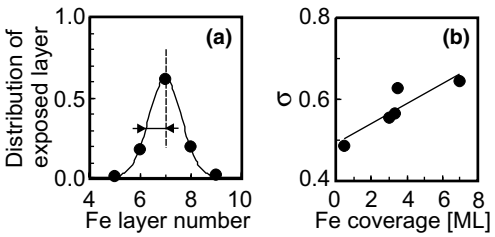

Fig. 3. (a) Distribution of exposed Fe layers at a coverage of 7 ML Fe. The half width at half maximum (HWHM), σ, is obtained from a Gaussian fit. (b) HWHM is plotted as a function of the Fe coverage. The line is a guide for the eye.

is now covered by 1 ML of Fe and small Fe islands appear on the second layer. For a coverage of 3 ML, up to three different layers are exposed on the surface as can be seen in Fig. 2(e), where the second, the third, and the fourth Fe layers are observed. Fig. 2(f) was obtained after the deposition of 7 ML of Fe. It is still possible to recognize the Mn(001) surface morphology. On this film up to five different layers of Fe are exposed and there are no 3D Fe islands present on the surface.

In order to elucidate if there is a change in the growth mode with the thickness we measured the distribution of exposed Fe layers for various Fe coverages [17]. We fitted the distribution of exposed Fe layer using a Gaussian curve (Fig. 3(a)). The half width at half maximum (σ) is plotted as function of the nominal coverage (Fig. 3(b)). There is a linear increase of σ as a function of Fe coverage but there is no drastic variation. From this analysis we can conclude that the growth of Fe on Mn(001) is almost layer-by-layer.

3.3. Atomically and chemically resolved STM images

Fig. 4 shows atomically and chemically resolved STM images. Fig. 4(a) was measured on the Fe(001) surface. In this image, besides a faint square lattice randomly distributed depressions can be seen at the atomic lattice sites. In a theoretical and experimental work, Hofer et al. studied the atomic corrugation obtained by STM on the Fe(001) surface [18]. They used the oxygen contaminants as a marker to identify the atomic

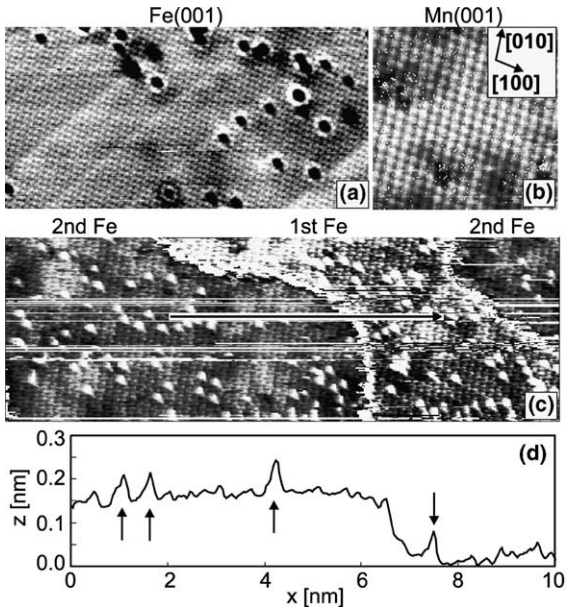

Fig. 4. Atomically and chemically resolved STM images obtained on a Fe(001) surface, a Mn(001) surface and on 1.5 ML Fe on Mn(001). (a) Fe(001) clean surface, 19×8 nm^2. Few black holes at atomic positions are clearly seen. The diagonal lines that run from the lower left corner to the upper right one are electrical noise. (b) Image measured on a Mn(001) surface covered with 0.2 ML Fe: 5×5 nm^2, $V_S = -0.1$ V, $I = 0.5$ nA. (c) was obtained on a 1.5 ML Fe film: 20×6.7 nm^2, $V_S = -2$ mV, $I = 9.8$ nA. The gray scale has been adjusted in every terrace in order to enhance the contrast between the Mn atoms and the Fe atoms. (d) Profile measured along the line shown in panel (c), the position of the Mn atoms are marked by arrows. The close-packed directions are shown in (b). The images are slightly distorted by thermal drift (~0.3 nm/min). The in-plane lattice constants along the [100] and the [100] directions in the Mn and the Fe layers are the same as the lattice constant of Fe(001).

positions and to study the changes in the atomic corrugation of the Fe atoms as a function of the tip sample distance. For all the set points used in their experiments and calculations, the oxygen atoms always appears like depressions. The concentration of these depressions is about 1% and is constant for all the films that we have studied. As mentioned before, around 1% oxygen contaminants were measured by Auger spectroscopy on the clean Fe whisker. Therefore, we tentatively identify these depressions as oxygen atoms adsorbed on the surface. Later on, measuring $I(V)$

curves on these defects we will confirm this assumption.

Fig. 4(b) was measured on the Mn(0 0 1) surface after the deposition of 0.2 ML of Fe. In this image a square lattice is clearly seen and two different types of lattice positions can be distinguished. Most of the atomic positions appear bright and few of them appear dark. Contrary to the previous case, the number of these dark atomic positions increases with the amount of Fe deposited, while we had checked by Auger that the oxygen signal stays constant during the Fe deposition. Fig. 4(c) was obtained after depositing 1.5 ML of Fe at room temperature. With this amount of Fe, the Mn surface is covered with a complete layer of Fe and in some areas the second layer can be seen as is shown in Fig. 4(c). In contrast with the image shown in Fig. 4(b), at this coverage most of the atomic positions are dark and a small percentage, that depends on the Fe thickness, is bright. The concentration of these bright atomic positions is $12 \pm 2\%$ for the first Fe layer and $7 \pm 1\%$ for the second Fe layer as measured from the atomically and chemically resolved images as the one shown in Fig. 4(c). In Fig. 4(d) a line profile taken in Fig. 4(c), four bright atomic positions are seen. The corrugation of this bright sites is 50 pm and the full width at half maximum (FWHM) is 0.17 nm. We can compare these values with the values obtained in two different experimental systems like Pb/Cu(1 1 1) [19] where the Pb atoms are embedded in the Cu(1 1 1) surface and the apparent corrugation is 70 pm and the FWHM is 0.20 nm and Fe/Pt(1 1 1) where the Fe atoms are adsorbed on the surface and present an apparent height of 0.12 nm and a FWHM of 0.7 nm [20]. We can conclude that the bright spots correspond to foreign atoms embedded in the surface and not to atoms adsorbed on the surface. If we consider also the decrease in the number of these bright atoms with the increase in the Fe deposited and the contrast between Mn and Fe found in our previous experiments on the growth of Mn on the Fe(0 0 1) surface [10], we tentatively identify them as Mn atoms.

In order to identify better the nature of these features we measured $I(V)$ curves on every pixel of the topographic images. In Fig. 5(a) we show a STM topography measured on a Mn(0 0 1) surface covered with 0.2 ML of Fe. As we have shown before (Fig. 2(b) and (c)) the deposition of submonolayer amounts of Fe leads to the formation of monoatomic high islands. The Fe islands present on the surface are labelled as 1 ML Fe. In Fig. 5(c) we show the value of the $I(V)$ curve at +0.3 V. From this image it is clear that after the deposition of 0.2 ML of Fe the Mn substrate and the deposited Fe island are far from been homogeneous in composition.

The $\mathrm{d}I/\mathrm{d}V$ curves measured on this area are plotted in panels (e) and (f) of Fig. 5. In panel (e) of Fig. 5 we show the $\mathrm{d}I/\mathrm{d}V$ curves measured on the bright areas of the Fe island (solid black curve) and on the grey areas on the Mn terrace (solid grey curve). With the help of our previous experiments and theoretical calculations on the Mn films grown on Fe(0 0 1) whiskers we can identify one of the $\mathrm{d}I/\mathrm{d}V$ curves as originated from the Mn(0 0 1) electronic structure [9]. It has been shown that the $\mathrm{d}I/\mathrm{d}V$ curves measured on the Mn(0 0 1) surface always present a dip at +0.1 V (grey arrow in Fig. 5(e) and (f)). The $\mathrm{d}I/\mathrm{d}V$ curves measured on the Fe areas present a shoulder at +0.3 V. Therefore, the dark areas in panels (b)–(d) of Fig. 5 correspond to the Mn atoms present on the surface (grey solid curve in panels (e) and (f) in Fig. 5) and accordingly the bright spots corresponds to the Fe positions (black solid curve in panels (e) and (f) in Fig. 5). For comparison we included in Fig. 5(f) (dashed black curve) the $\mathrm{d}I/\mathrm{d}V$ curve taken on one of the impurities present on the surface, as the ones shown in Fig. 4(a). This curve does not show any of the characteristic signatures found on the Mn and Fe curves [10]. Panels (b)–(d) in Fig. 5 are constructed with the value of the tunnelling current for three different values of the bias voltage. It is clear that the position and contrast between bright and dark spots are perfectly preserved in the three panels. These spectroscopic measurements proof that the surface is not homogeneous and it is composed by Mn and Fe atoms.

Once we have been able to identify the chemical identity of the features observed on the surface of the different films we proceed to estimate the relative abundance. We found that the first layer consists of 12% of Mn and 88% of Fe. The second

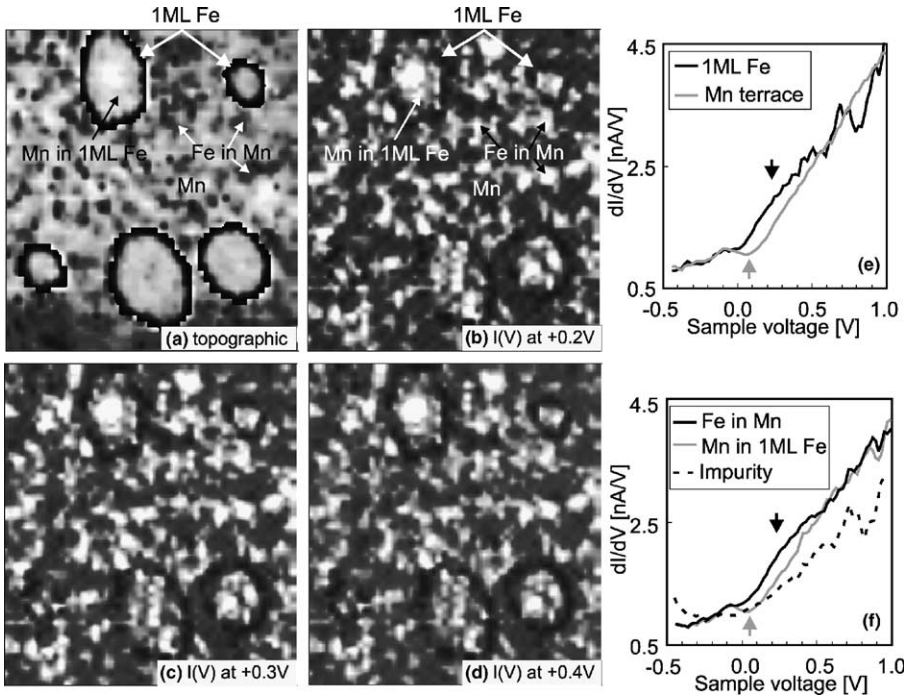

Fig. 5. (a) STM image of 0.2 ML of Fe deposited on Mn(001) at RT, 20×22 nm^2 taken with $V_S = -0.5$ V and $I = 0.5$ nA. (b)–(d) Images constructed with the value of the $I(V)$ curves at +0.2, +0.3 and +0.4 V respectively measured in every pixel of the image shown in panel (a). (e) dI/dV curves obtained from the $I(V)$ curves measured in the Fe island (black solid line) and in the Mn substrate (solid gray line). (f) dI/dV curves obtained from the $I(V)$ curves measured in the spots marked in the STM image in panel (a).

layer consists of 7% of Mn and 93% of Fe. These observations are consistent with the Auger measurements that show a decrease on the amplitude of the Mn(40 eV) peak with the Fe coverage. In summary, from the observations of the atomically and chemically resolved STM images, Auger spectroscopy and STS data we can conclude that for Fe films grown on Mn(001) at RT, the intermixing between Mn and Fe decreases with the increase in the Fe thickness and it is observable for the first four layers.

3.4. Geometric structure of the Fe layers

In order to determine the geometric structure of the Fe layers we measured the in-plane and out-of-plane distances with the STM. In a previous work [10] we had shown that Mn films grown pseudomorphically on Fe(001), having a bct structure with the same in-plane lattice constant than the Fe(001), i.e. 0.287 nm. An atomically resolved image of such a surface can be seen in Fig. 4(b). The Fe films deposited on these Mn(001) surfaces also grown pseudomorphically, presenting the same in-plane lattice constant than the bcc Fe(001) surface.

We measured the apparent step height for different Fe layers as a function of sample bias voltage. We did the measurements in this way to rule out any influence due to changes in the electronic structure of the films with the thickness. The heights were obtained from histograms of plane fitted STM images taken at different bias voltages. Fig. 6(a) shows one of these STM images measured at $V = -1.0$ V. In Fig. 6(b) we show the histogram of heights present on the image of panel (a). By measuring the distance between the peaks we can determine the height of the steps present on the image. We took the half width at half maximum as error bar for the step heights values. This method for measuring the steps heights is more

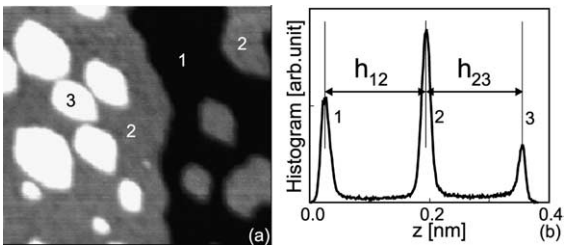

Fig. 6. (a) STM image of 1.5 ML of Fe deposited on a Mn(001) substrate at RT, 50×45 nm^2, measured at $V_S = -1.0$ V and $I = 0.04$ nA. (b) Histogram showing the heights distributions present in the image of panel (a). By measuring the distance between the peaks in the histogram we obtain the step height. The numbers on the STM image do not represent the Fe thickness.

accurate than making individual line profiles across the steps.

Fig. 7(a)–(e) correspond to h_{01}, h_{12}, h_{23}, h_{34}, and h_{67}, h_{78}, respectively. h_{ij} denotes the interlayer distance between layers i and j. The step height does not show a strong dependence on the sample bias voltage, but changes slightly with the thickness. h_{01} and h_{12} scatter around 0.160 ± 0.007 nm. h_{23} is slightly higher ($\sim 0.165 \pm 0.007$ nm), but almost the same as h_{01} and h_{12}. h_{34} is around 0.155 ± 0.007 nm. Above the fourth layer the interlayer distances are around 0.145 ± 0.007 nm as shown in Fig. 7(e).

The averaged values of h_{ij}'s below the Fermi level taken from panels (a)–(e) of Fig. 7 are plotted in Fig. 7(f). [2] This figure shows clearly that there is a change in the step height with the Fe thickness. The first, the second, and the third Fe layer have the same step height: 0.162 ± 0.007 nm. The fourth Fe layer has a lower step height: 0.155 ± 0.007 nm. Then, the Fe film above the fourth layer has an equivalent interlayer distance of 0.145 nm $\pm$ 0.007 nm. In the studies of bct-Fe_xMn_{1-x}/Ir(001) superlattices [21], a sharp change of the interlayer distance was observed from 0.165 ± 0.001 nm for $Fe_{0.7}Mn_{0.3}$ to 0.153 ± 0.001 nm for $Fe_{0.9}Mn_{0.1}$ by X-ray diffraction measurements. In that work the authors linked the reduction in the Mn percentage in the films with the change in the interlayer distance. It is worth to mention that STM is not the best technique to get precise crystallographic information because the step height measured can be affected by changes in the electronic structure between different layers and also by changes in the work function. In our case the former has been excluded by measuring the apparent step height at different bias voltages but with our experimental data the later cannot be excluded. Therefore, from these step height measurements we can conclude that for Fe films thicker than four layers, the Fe film presents a bcc structure. For the first four layers we can tentatively conclude that the interlayer distance is different.

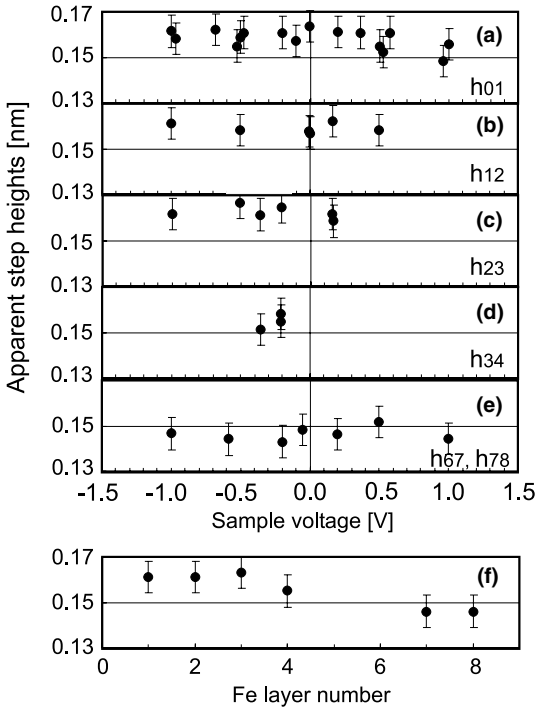

Fig. 7. (a)–(e) Apparent step heights of the Fe layers as a function of the sample bias voltage. h_{ij} indicates the step height between layers i and j. Since the heights are independent of the current, the height at each voltage is obtained from the STM images measured at current set points between 0.02 and 1 nA. (f) shows the interlayer distances obtained at negative voltages [2].

3.5. STS measurements on the Fe layers

Using the spectroscopic capabilities of the STM we studied the surface electronic structure of the

[2] Since the dI/dV curves are featureless for negative bias voltages, we expect smaller electronic effects.

Fe layers. STS measurements were performed in the following way. $I(V)$ curves were obtained at every pixel of a constant current topographic image by opening the STM feedback loop. $\mathrm{d}I/\mathrm{d}V$ curves were obtained by numerical differentiation of the $I(V)$ curves.

We will first focus on the electronic structure of the thick Fe films. As we have shown before Fe films thicker than four layers present a bcc structure with a lattice parameter that corresponds to bulk Fe. We also know that for these thick films there is no intermixing with the atoms from the substrate. Fig. 8 was obtained on a 7 ML Fe film. As was explained before, with the increase of the Fe thickness, the number of exposed layers increases and therefore the surface becomes rougher (Fig. 8(a)). For a 7 ML Fe film four Fe layers are exposed. All these layers reveal the same $\mathrm{d}I/\mathrm{d}V$ curve that presents a clear peak at +0.2 V (Fig. 8(b)). The presence of this peak in the STS spectra measured on the surface of the Fe(0 0 1) whisker was first described by Stroscio et al. [11]. With the help of a theoretical calculation they traced the origin of this peak back to a nearly unperturbed d orbital. The $\mathrm{d}I/\mathrm{d}V$ curves shown in Fig. 8(b) are identical to the ones that we measured on a Fe(0 0 1) whisker [14].

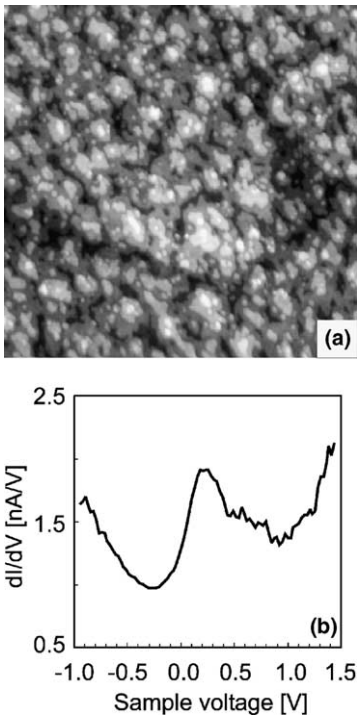

Fig. 8. (a) STM topographic image obtained on the Mn layers covered by about 7 ML Fe ($V_S = -0.5$ V, $I = 0.5$ nA (90×90 nm^2)). About four Fe layers are exposed. At this area spectroscopy measurements were performed. (b) shows an averaged $\mathrm{d}I/\mathrm{d}V$ curve. A peak at +0.2 V is visible.

The situation for the first four Fe layer is more complicated because, as we have shown before in this paper, there is intermixing between Fe and Mn that changes from layer to layer. In order to retrieve the surface density of states the $\mathrm{d}I/\mathrm{d}V$ curves were normalized. We used the curves measured on the thick Fe layers as a reference during the normalization procedure. Following the method proposed by Ukraintsev [22], we fitted the exponential background of the $\mathrm{d}I/\mathrm{d}V$ curves with a function T, and then we used this function to normalize the $\mathrm{d}I/\mathrm{d}V$ curves. Fig. 9(a) shows a representative $\mathrm{d}I/\mathrm{d}V$ curve for the four first layers of Fe on Mn(0 0 1) (solid curve). The $\mathrm{d}I/\mathrm{d}V$ curve shows two shoulders at +0.2 and ~+1.7 V. For negative and higher (>+2 V) positive voltages the $\mathrm{d}I/\mathrm{d}V$ curve increases exponentially. This energy range was used to fit the exponential background (T) (grey dashed curve in Fig. 9(a)). In Fig. 9(b) we show the normalized conductance $((\mathrm{d}I/\mathrm{d}V)/T)$ curve (black curve). In the normalized conductance the two shoulders that appear in the $\mathrm{d}I/\mathrm{d}V$ curves show up as two peaks. In order to determine the position in energy of these two peaks we fit the normalized conductance with two Gaussian curves that are shown in Fig. 9(b) (grey curve). From this fit we found that the energy position of the two peaks is $+0.3\pm0.1$ V and $+1.0\pm0.1$ V.

Figs. 8(b) and 9(c) show the tunneling conductance ($\mathrm{d}I/\mathrm{d}V$) obtained on an Fe film thicker than four layers. In this case the $\mathrm{d}I/\mathrm{d}V$ curve shows a peak at 0.2 V above the Fermi level. Following the same procedure described above we just fit the exponential background of the $\mathrm{d}I/\mathrm{d}V$ curve (grey dashed curve in Fig. 9(c)). Fig. 9(d) shows the normalized tunneling conductance $((\mathrm{d}I/\mathrm{d}V)/T)$ with a solid curve and using a Gaussian curve we determined the energy position of the peak present in the spectra (grey solid curve in Fig. 9(d)). We found that the energy position is 0.2 V above the

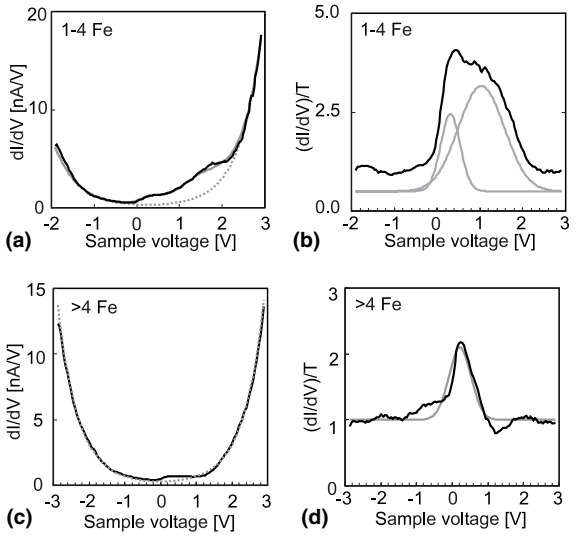

Fig. 9. (a) The dI/dV curve obtained on the first four Fe layers (black solid curve) was normalized by a fitted tunneling probability function (T) (grey dashed curve). The grey solid curve in (a) denotes a fitted dI/dV curve. (b) $(dI/dV)/T$ curve (black solid curve) shows a broad peak in the energy range between the Fermi level and +2.5 V, it can be fitted with two Gaussian curves (grey solid curve) centered in energy at $+0.3 \pm 0.1$ V and 1.0 ± 0.1 V respectively. (c) The dI/dV curve obtained on the Fe film thicker than four layer (black solid curve) was normalized by a fitted T (grey dashed curve). (d) $(dI/dV)/T$ curve (black solid curve) shows a peak at 0.2 V above the Fermi level. It can be fitted by a single Gaussian curve (grey solid curve). (a) and (c) were measured at set points of $V_S = -0.6$ V, $I = 0.3$ nA and $V_S = -0.5$ V, $I = 0.5$ nA, respectively.

Fermi level, this energy corresponds to the energy of the surface state of bcc Fe(0 0 1) [11].

According to the above observations, we conclude that (1) the first four Fe layers (which have a bct structure and include intermixed Mn) show peaks at $+0.3 \pm 0.1$ V and $+1.0 \pm 0.1$ V in the density of states ($(dI/dV)/T$); (2) the Fe layers (>4 ML) (which have a bcc structure and do not contain intermixed Mn) show a peak at +0.2 V in the density of states ($(dI/dV)/T$).

4. Conclusion

In this study we investigated the geometric structure, the concentration of the intermixed Mn atoms, and density of states for the Fe/Mn magnetic multilayer film with STM, STS, and Auger spectroscopy. The Fe film grows almost layer-by-layer. The in-plane lattice constant is the same as bcc-Fe(0 0 1). Intermixing Mn atoms were observed with a concentration of $12 \pm 2\%$ for the first and $7 \pm 1\%$ for the second Fe layer. The concentration of Mn was found to decrease with an increase of the number of Fe layers. Interlayer apparent distances of 0.161 ± 0.007 nm for the first and the second layer, 0.163 ± 0.007 nm for the third layer, 0.155 ± 0.007 nm for the fourth, and 0.145 ± 0.007 nm for thicker Fe layers were found. From this it follows that Fe film thicker than four layers grow in a bcc structure and we can tentatively conclude that the first four Fe layers grow in a bct one. The surface density of states of the Fe layers show that: (1) the first four Fe layers have peaks around $+0.3 \pm 0.1$ V and $+1.0 \pm 0.1$ V; (2) the Fe film thicker than four layers has one peak at +0.2 V, which energy corresponds to the bcc-Fe(0 0 1) surface state energy.

One can conclude that around the fourth layer both the electronic structure and the interlayer distance change. We attribute these change to the relaxing of the Fe film from a bct to a bcc structure. The onset of this structural transition is probably related to the intermixing behavior at the Fe/Mn interface [21].

This indicates that in typical magnetic multilayer films some monolayers at the interface have different geometric and electronic structures. This might cause different magnetic structure at the interface of the magnetic multilayer films.

Acknowledgements

This work was supported by the Stichting voor Fundamenteel Onderzoek der Materie (FOM), which is funded by the Nederlandse Organisatie voor Wetenschappelijk Onderzoek (NWO), and the European Growth Project MAGNETUDE. We are especially grateful to D.T. Pierce for supplying us with the Fe whiskers. One of us, ALVP, thanks the Nederlandse Organisatie voor Wetenschappelijk Onderzoek (NWO) and Ministerio de Ciencia y Tecnología for the financial support.

References

[1] S.A. Wolf, D.D. Awschalom, R.A. Buhrman, J.M. Daughton, S. von Molnar, M.L. Roukes, A.Y. Chtchelkanova, D.M. Treger, Science 294 (2001) 1488.
[2] S. Yuasa, T. Nagahara, Y. Suzuki, Science 297 (2002) 234.
[3] J. Shen, J. Kirschner, Surf. Sci. 500 (2002) 300.
[4] A. Cebollada, R.F.C. Farrow, M.F. Toney, Nanostructured Magnetic Materials, in: S. Bandyopadhayay, H.S. Nalwa, American Scientific Publishers, 2002, p. 93.
[5] J. Unguris, R.J. Celotta, D.A. Tulchinsky, D.T. Pierce, J. Magn. Magn. Mater. 198–199 (1999) 396.
[6] D.A. Tulchinsky, J. Unguris, R.J. Celotta, J. Magn. Magn. Mater. 212 (2000) 91.
[7] D.T. Pierce, A.D. Davies, J.A. Stroscio, D.A. Tulchinsky, J. Unguris, R.J. Celotta, J. Magn. Magn. Mater. 222 (2000) 13.
[8] R. Schäfer, R. Urban, D. Ullmann, H.L. Meyerheim, B. Heinrich, L. Schultz, J. Kirschner, Phys. Rev. B 65 (2002) 144405.
[9] T.K. Yamada, M.M.J. Bischoff, G.M.M. Heijnen, T. Mizoguchi, H. van Kempen, Phys. Rev. Lett. 90 (2003) 056803.
[10] T.K. Yamada, M.M.J. Bischoff, T. Mizoguchi, H. van Kempen, Surf. Sci. 516 (2002) 179.
[11] J.A. Stroscio, D.T. Pierce, A. Davies, R.J. Celotta, Phys. Rev. Lett. 75 (1995) 2960.
[12] M.M.J. Bischoff, Ph.D. thesis, University of Nijmegen, 2002.
[13] R.N. Gardner, J. Crys. Grow. 43 (1978) 425.
[14] M.M.J. Bischoff, T.K. Yamada, C.M. Fang, R.A. de Groot, H. van Kempen, Phys. Rev. B 68 (2003) 045422.
[15] H. Ardhuin, K. Suenaga, M.J. Casanove, E. Snoeck, C. Colliex, H. Fischer, S. Andrieu, M. Piecuch, Phys. Rev. B 58 (1998) 14135.
[16] A. Zangwill, Physics at Surfaces, Cambridge, p. 21.
[17] D.T. Pierce, J.A. Stroscio, J. Unguris, R.J. Celotta, Phys. Rev. B 49 (1994) 14564.
[18] W.A. Hofer, J. Redinger, A. Biedermann, P. Varga, Surf. Sci. 466 (2000) L795.
[19] C. Nagl, O. Haller, E. Platzgummer, M. Schmidt, P. Varga, Surf. Sci. 321 (1994) 237.
[20] M.F. Crommie, C.P. Lutz, D.M. Eigler, Phys. Rev. B 48 (1993) 2851.
[21] A. Dechelette-Barbara, J.M. Tonnerre, M.C. Saint-Lager, F. Bartolome, J.F. Berar, D. Raoux, H.M. Fischer, M. Piecuch, V. Chakarian, C.C. Kao, M. Gailhanou, S. Lefèvre, M. Bessière, J. Magn. Magn. Mater. 165 (1997) 87.
[22] V.A. Ukraintsev, Phys. Rev. B 53 (1996) 11176.